

A twelve-quadrupole correction for the interaction regions of high-energy accelerators

Javier Fernando Cardona,^{1,*} Yohany Rodríguez García,^{1,2} and Rogelio Tomás García³

¹*Universidad Nacional de Colombia, Bogotá, Colombia*

²*Universidad Antonio Nariño, Bogotá, Colombia*

³*CERN, Geneva CH-1211, Switzerland*

(Dated: February 17, 2020)

Corrections of gradient errors in the interactions regions (IRs) of high energy colliders have traditionally been made by changing the strengths of quadrupoles that are common to both beams, such as the triplet quadrupoles. This article shows that magnetic errors in the IR quadrupoles that are not common to both beams, such as the matching quadrupoles, can have an important influence and, therefore, the correction should also include these quadrupoles. A correction based on twelve IR quadrupoles (common and no common) is presented and validated through MADX simulations. To estimate the strengths of this correction, the action and phase in the inter-triplet space, the space that separates the two triplets of the IR, are required. A novel method to estimate these quantities is also presented. The main sources of uncertainties in this novel method are identified and compared to the current method that uses two beam position monitors within the inter-triplet space. Finally, LHC experimental data is used to estimate the strengths of a twelve-quadrupole correction in the interaction region 1 of the LHC. The resulting correction is compared with a six-quadrupole correction estimated with another method called segment-by-segment (SBS).

PACS numbers: 41.85.-p, 29.27.Eg, 29.20.db

I. INTRODUCTION

Gradient errors in the interaction regions (IRs) produce the largest deviations in the optical model of a high-energy accelerator. The correction of these errors is not only relevant to the overall performance of the machine but also to ensure the best quality of the beam at the interaction point (IP).

The ideal correction procedure is to measure the individual gradient errors of each IR magnet and change their strengths to exactly compensate for each gradient error. However, there is still no method to determine magnetic errors individually for each IR quadrupole. Current correction methods vary the strength of a few IR quadrupoles in hopes of suppressing the effect of all gradient errors present in the IR. The first correction of this nature used in the LHC varied the strengths of two IR quadrupoles. These strengths can be estimated with two different methods, which are segment-by-segment (SBS) [1–4] and action and phase jump analysis (APJ) [5, 6], and both of them give similar results. The two-quadrupole correction is effective in suppressing the β beating in the arcs. However, suppression of the β beating in the IP is not guaranteed. To solve this problem, two different corrections were proposed. The first is a six-quadrupole correction with strengths that can be estimated with SBS [7] and the second is a four-quadrupole correction with strengths that can be estimated with APJ [6]. It can be demonstrated that these two corrections are also equivalent and both of them effectively suppress the β -beating in the arcs and the IP as well. However, these corrections work only if the magnetic errors in

the matching quadrupoles, the quadrupoles that are just outside the triplets, are small. Otherwise, a more general correction is required. In this paper, a twelve-quadrupole correction, which includes matching quadrupoles, is presented and validated through MADX [8] simulations and experimental data.

Estimates of corrector strengths in this paper are based on APJ and, particularly, they depend on the action and phase in the inter-triplet space, the space that separates the two triplets of the IR. The current method to estimate these quantities do not have sufficient accuracy to allow reliable estimates of the correction strengths. A novel method to estimate action and phase in the inter-triplet space with very low uncertainties is presented in this paper.

The paper starts with a review of the APJ method in Sec. II. Then, in Sec. III, the novel method to estimate the action and phase in the inter-triplet space is described. It is shown that this new method has significantly smaller uncertainties than the uncertainties associated with the current method that uses two BPMs in the inter-triplet space. This new method uses k -modulation measurements and the action and phase that are independent of the longitudinal position s : the action and phase constants. Sec. IV describes how these constants can be measured accurately. Applying this new development to LHC experimental data, the strengths of a correction that uses only common quadrupoles are estimated in Sec. V. Comparisons between the strengths obtained from beam 1 data and beam 2 data suggest that magnetic errors in the no common quadrupoles are significant, which leads to the more general twelve-quadrupole correction mentioned earlier. This correction is introduced and tested with simulations in Sec. VI. Finally, the strengths of a twelve-quadrupole correction are

* jfcardona@unal.edu.co

estimated from experimental LHC turn-by-turn (TBT) data and compared with a six-quadrupole correction estimated with SBS in Sec. VII.

II. THE ACTION AND PHASE JUMP METHOD

It has been shown in [6, 9] that the APJ method allows the mathematical description of a one-turn particle trajectory in the presence of linear magnetic errors with

$$z(s) = \sqrt{2J(s)\beta_n(s)} \sin[\psi_n(s) - \delta(s)], \quad (1)$$

where $z(s)$ is the particle transverse position (either x or y) with respect to the closed orbit, $\beta_n(s)$ and $\psi_n(s)$ are the nominal lattice functions, and $J(s)$ and $\delta(s)$ are the actions and phases that, unlike the action and phase of the conventional betatron equation, jump at magnetic error locations.

These jumps allow to estimate the deflection θ , also called magnetic kick, that a particular magnetic error produces in the particle trajectory with

$$|\theta| = \sqrt{\frac{2J_0 + 2J_1 + 4J_0J_1 \cos(\delta_1 - \delta_0)}{\beta_n(s_e)}}, \quad (2)$$

where J_0 , J_1 , δ_0 , and δ_1 correspond to the actions and phases immediately to the left and to the right of s_e , the axial location of the magnetic error. Assuming that the magnetic error has only quadrupole components, the following relationships are valid

$$\theta_x = -B_{1x}x_e + A_{1y}y_e, \quad (3a)$$

$$\theta_y = B_{1y}y_e + A_{1x}x_e, \quad (3b)$$

where B_1 and A_1 are quantities proportional to the normal and the skew quadrupole components of the magnetic error that caused the deflection of the particle trajectory, and x_e and y_e correspond to the position of the particle evaluated at s_e . Since the deflections in both planes can be estimated with Eq. (2), it is also possible to estimate the numerical values of B_1 and A_1 using Eq. (3).

In practice, J and δ at a particular location in the accelerator are estimated using the trajectory measurements of two adjacent BPMs, i and $i + 1$, as follows:

$$J_{i+1} = \frac{(z_i/\sqrt{\beta_{ni}})^2 + (z_{i+1}/\sqrt{\beta_{ni+1}})^2}{2 \sin^2(\psi_{ni+1} - \psi_{ni})} - \frac{z_i z_{i+1} \cos(\psi_{ni+1} - \psi_{ni})}{\sqrt{\beta_{ni}\beta_{ni+1}} \sin^2(\psi_{ni+1} - \psi_{ni})}, \quad (4)$$

and

$$\tan \delta_{i+1} = \frac{(z_i/\sqrt{\beta_{ni}}) \sin \psi_{ni+1} - (z_{i+1}/\sqrt{\beta_{ni+1}}) \sin \psi_{ni}}{(z_i/\sqrt{\beta_{ni}}) \cos \psi_{ni+1} - (z_{i+1}/\sqrt{\beta_{ni+1}}) \cos \psi_{ni}}. \quad (5)$$

This process is repeated for all adjacent BPM pairs in the accelerator, which makes possible to find J and δ as function of s . Because the number of BPMs is limited, it is not possible to estimate the actions and phases associated with every accelerator magnet. Only the actions and phases associated with certain group of magnets can be estimated. In the LHC, for example, the actions and phases immediately to the left and right of the high luminosity IRs can be easily identified, as seen in Fig. 1 of [6]. Although these actions and phases are not sufficient to estimate the deflections produced by every individual error in the magnets within a particular IR, it is possible to estimate an equivalent magnetic kick for the entire IR using Eq. (2). Similar to the kick of a magnetic error, the equivalent kick can also be expressed based on its magnetic quadrupole components $B_{1x,e}$, $B_{1y,e}$, and $A_{1,e}$, as follows:

$$\theta_{x,e} = -B_{1x,e}x_e + A_{1,e}y_e, \quad (6a)$$

$$\theta_{y,e} = B_{1y,e}y_e + A_{1,e}x_e. \quad (6b)$$

If Eq. (6) is used with two one-turn beam trajectories, it is possible to estimate the quadrupole components of the equivalent kick as

$$B_{1x,e} = \frac{y_{e1}\theta_{x2,e} - y_{e2}\theta_{x1,e}}{x_{e1}y_{e2} - x_{e2}y_{e1}}, \quad (7a)$$

$$B_{1y,e} = \frac{x_{e1}\theta_{y2,e} - x_{e2}\theta_{y1,e}}{x_{e1}y_{e2} - x_{e2}y_{e1}}, \quad (7b)$$

$$A_{1,e} = \frac{x_{e1}\theta_{x2,e} - x_{e2}\theta_{x1,e}}{x_{e1}y_{e2} - x_{e2}y_{e1}}, \quad (7c)$$

where the numerical subscripts are used to differentiate variables that belong to one trajectory or the other.

The quadrupole components of the equivalent kick can be used to estimate a correction that suppresses the effect of all magnetic errors in the IR. For the normal quadrupole errors, this suppression is achieved by changing the strength of two out of the six normal IR quadrupoles so that that the equivalent kick generated by these strengths has quadrupole components $B_{1x}^{(c)}$ and $B_{1y}^{(c)}$ that are equal but opposite to the quadrupole components of the original equivalent kick. This leads to

$$B_{1z,e} = -B_{1z}^{(c)}, \quad (8)$$

and

$$B_{1x,e} = -\frac{\Delta K_{1a}I_{x,a} + \Delta K_{1b}I_{x,b}}{\beta_{n,x}(s_e)}, \quad (9a)$$

$$B_{1y,e} = -\frac{\Delta K_{1a}I_{y,a} + \Delta K_{1b}I_{y,b}}{\beta_{n,y}(s_e)}, \quad (9b)$$

where the measured quadrupole components of the equivalent kick have been related to the strength changes ΔK_{1a} and ΔK_{1b} needed in quadrupoles a and b to suppress the effect of the normal quadrupole errors present in the IR. Also in these equations, $\beta_{n,z}$ (with z representing either the x or the y plane) represent the nominal β

functions, and $I_{z,i}$ corresponds to the integrals defined by

$$I_{z,i} = \int_{s_{li}}^{s_{ri}} ds' \beta_{n,z}(s'), \quad (10)$$

where s_{li} and s_{ri} are the longitudinal positions of the left and right sides of magnet i , which can be either a or b .

The strengths ΔK_{1a} and ΔK_{1b} can be found by inverting Eq. (9) resulting in

$$\Delta K_{1a} = \frac{B_{1y,e}\beta_{n,y}(s_e)I_{x,b} - B_{1x,e}\beta_{n,x}(s_e)I_{y,b}}{I_{x,a}I_{y,b} - I_{x,b}I_{y,a}}, \quad (11a)$$

$$\Delta K_{1b} = \frac{B_{1x,e}\beta_{n,x}(s_e)I_{y,a} - B_{1y,e}\beta_{n,y}(s_e)I_{x,a}}{I_{x,a}I_{y,b} - I_{x,b}I_{y,a}}. \quad (11b)$$

One of the effects produced by normal quadrupole errors present in a particular IR is β -beating. When only two IR quadrupoles are used for correction, with strengths estimated with Eq. (11), the β -beating is effectively suppressed everywhere in the ring. The suppression, however, is not complete; a significant β -beating can still remain in the IP as shown with the red curve in Fig. 7 of [6].

To solve this problem, the IR magnets can be divided in two groups: the left triplet magnets and the right triplet magnets. If the action and phase in the inter-triplet space can be known, the equivalent kicks corresponding to each triplet can be estimated. Therefore, two strengths can be estimated for each triplet with Eq. (11). This leads to a correction with four quadrupole per IR instead of two per IR, which effectively suppress the β -beating everywhere in the ring including the IP as shown with the blue curve in Fig. 7 of [6].

III. ACTION AND PHASE IN THE INTER-TRIPLET SPACE

The action and phase in the inter-triplet space is currently obtained with the two BPMs closest to the IP (BPMSWs) using Eqs. (4) and (5). This method does not have sufficient accuracy to allow reliable estimates of the correction strengths. A novel method to estimate these quantities is presented in this section.

Assume that IR1 of the LHC is been configured as a high luminosity IR with a $\beta^* = 40$ cm (β^* is the value of the β -function at the IP). Also assume that magnetic quadrupole errors are present only in the IR. If a one-turn particle trajectory is generated with this LHC lattice, the corresponding APJ description, derived from Eq. (1), is

$$z(s) = \begin{cases} \sqrt{2J_0\beta_n(s)} \sin[\psi_n(s) - \delta_0] & \text{arc left of IR1} \\ \sqrt{2J_t\beta_n(s)} \sin[\psi_n(s) - \delta_t] & \text{inter-triplet space} \\ \sqrt{2J_1\beta_n(s)} \sin[\psi_n(s) - \delta_1] & \text{arc right of IR1} \end{cases} \quad (12)$$

where $\beta_n(s)$ and $\psi_n(s)$ correspond to the nominal lattice functions while J and δ correspond to the actions and phases used in APJ analysis. The subscripts 0 and 1 are used to label variables in the arc that are to the left and to the right of IR1 respectively. The subscript t is used to label variables corresponding to the inter-triplet space (see also Fig. 1).

It is also possible to use the conventional betatron equation to mathematically describe the same one-turn particle trajectory as follows

$$z(s) = \sqrt{2J_c\beta_r(s)} \sin[\psi_r(s) - \delta_c], \quad (13)$$

where $\beta_r(s)$ and $\psi_r(s)$ are the lattice functions that include magnetic errors and J_c and δ_c are the action and phase constants.

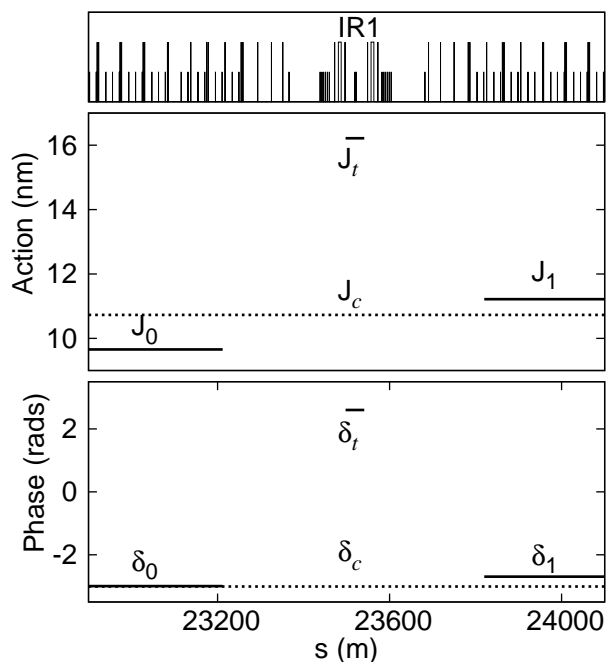


FIG. 1. The action and phase variables used in APJ analysis (solid lines) are illustrated, as well as the action and phase constants (dotted lines). All the actions and phases were obtained from a simulated average trajectory of the LHC (beam 1). In the upper part of the figure, the optical lattice is represented by long and short vertical bars corresponding to quadrupole and dipole magnets respectively. The two triplets of IR1 and the inter-triplet space can be seen just below the “IR1” label.

In the inter-triplet space Eqs. (12) and (13) lead to

$$\begin{aligned} z(s) &= \\ &= \sqrt{2J_c\beta_r(s)} \sin[\psi_r(s) - \delta_c] \\ &= \sqrt{2J_t\beta_n(s)} \sin[\psi_n(s) - \delta_t]. \end{aligned} \quad (14)$$

The beta and phase functions in the inter-triplet space are given by well-known analytical formulas. These formulas depend on the minimum value of beta function,

which is usually denoted by the symbol β_w , and the difference between the axial location of β_w and the axial location of the IP, which is generally known as the waist shift w . If these formulas are used in Eq. (14), the following relationships for the action and phase in the inter-triplet space can be deduced

$$J_t = J_c \frac{\beta_{w_n}}{\beta_{w_r}} \cos^2 \gamma_c (1 + \tan^2 \gamma_t), \quad (15)$$

and

$$\delta_t = \psi_n(s_t) + \arctan\left(\frac{L + w_n}{\beta_{w_n}}\right) - \gamma_t, \quad (16)$$

where

$$\tan \gamma_t = \frac{w_n - w_r + \beta_{w_r} \tan \gamma_c}{\beta_{w_n}}, \quad (17)$$

and

$$\gamma_c = \psi_r(s_t) + \arctan\left(\frac{L + w_r}{\beta_{w_r}}\right) - \delta_c. \quad (18)$$

In these expressions, the subscripts n and r are used to distinguish the nominal variables from variables associated to the lattice with errors, s_t corresponds to the axial location where the inter-triplet space starts, and L corresponds to half the length of the inter-triplet space.

Expressions (15) to (18) depend on experimental variables that are routinely obtained in the LHC [$\psi_r(s_t)$, w_r , and β_{w_r}] and variables that can be obtained directly from the nominal model of the accelerator [$\psi_n(s_t)$, w_n , β_{w_n} , and L]. In addition, they depend on the action and phase constants, which can be obtained from the experimental TBT data sets as shown in Sec. IV.

The three experimental variables required to estimate J_t and δ_t are obtained using two different techniques. To obtain β_{w_r} and w_r , a technique based on k -modulation is used [10]. The general idea of this technique is to change the strength of the two quadrupoles closest to the IP and record the corresponding changes of the betatron tunes in both planes. From this data, very accurate estimates of the average β functions of the two quadrupoles involved can be obtained. The values of β_{w_r} and w_r are obtained later through analytical equations that relate these variables with the average β functions.

To obtain the lattice functions with errors [$\beta_r(s)$ and $\psi_r(s)$], a technique based on Fourier analysis of TBT data is used [11]. In this technique the $\psi_r(s)$ functions are obtained directly from the phase resulting from the Fourier analysis in each BPM data set, while the $\beta_r(s)$ functions are obtained through equations that relate the phase advances between three consecutive BPMs and their nominal β functions.

The action and phase in the inter-triplet space can also be obtained using the two BPMs closest to the IP. Therefore, it is possible to test Eqs. (15) and (16) comparing the results of both methods. For this purpose simulated

TBT data is generated with MADX for a LHC lattice with quadrupole errors in IR1. In this simulation the “experimental values” β_{w_r} , w_r , and $\psi_r(s_t)$ are obtained directly from Twiss files generated by MADX for the lattice with errors while J_c and δ_c are obtained from the simulated TBT data. The four kinds of average max trajectories defined in [6] (see also Sec. VII) are obtained from the simulated TBT data, and J_t and δ_t are obtained for every trajectory using Eqs. (15) and (16) and also using the BPMSWs. In all cases there is an agreement of seven significant figures between the two methods for both quantities.

Since the uncertainties of all the experimental variables in Eqs. (15) and (16) are known (see Table I), the propagated uncertainties ΔJ_t and $\Delta \delta_t$ can be estimated. These uncertainties were estimated for the four average trajectories generated in the previous simulation. The maximum values are shown in the first row of Table II.

TABLE I. Uncertainties of the experimental variables required to estimate J_t and δ_t . The sources where these uncertainties were extracted are also listed.

Exp. Variable	Uncertainty	Extracted from:
$\psi_r(s_t)$	6 mrad	[12]
w_r	1 cm	k -modulation experiments
J_c	0.5 %	Sec. IV
δ_c	2 mrad	Sec. IV
β_{w_r}	0.3 mm	k -modulation experiments

TABLE II. Uncertainties associated with the estimates of action and phase in the inter-triplet space due to the uncertainties in Table I. These uncertainties are compared to the uncertainties of the method that uses 2 BPMSWs with a gain error of 1% in one of the BPMs.

Method	ΔJ_t (%)	$\Delta \delta_t$ (rads)
Eq. (15) and Eq. (16)	2.7	0.015
BPMSWs	32.0	0.164

For comparison purposes the uncertainties associated with the method using two BPMSWs are estimated. In this method BPM gain errors are the most important sources of uncertainty. Even assuming the best BPM calibration achieved in the LHC so far (1% gain error), the corresponding ΔJ_t and $\Delta \delta_t$ (second row of Table II) are significantly larger than the uncertainties associated with Eq. (15) and Eq. (16).

IV. ESTIMATING THE ACTION AND PHASE CONSTANTS

If one turn trajectories are well described by Eq. (13), J_c and δ_c can be estimated using, for example, Eqs. (4) and (5) with only one pair of BPMs. However, three

sources of known errors separate the experimental data from Eq. (13): electronic noise, uncertainties in the determination of the lattice functions with errors, and BPM gain errors.

The first source of errors can be avoided if average trajectories are used since this kind of trajectories have very low noise levels. The second source of errors has a small effect since the lattice functions with errors are currently determined with an accuracy of 1% [13, 14]. The third source of errors can have a significantly larger effect on the experimental data; it is the dominant source of the three types of errors. Fortunately, large gain errors are not an impediment to estimate accurately J_c and δ_c . Because Eqs. (4) and (5) allow finding a value of J_c and δ_c for every pair of adjacent BPMs in the ring, a large number of these measurements are available. If the differences between these measurements follow a Gaussian distribution, the averages values provide an accurate measurement of J_c and δ_c since their uncertainties should decrease as the square root of the number of measurements.

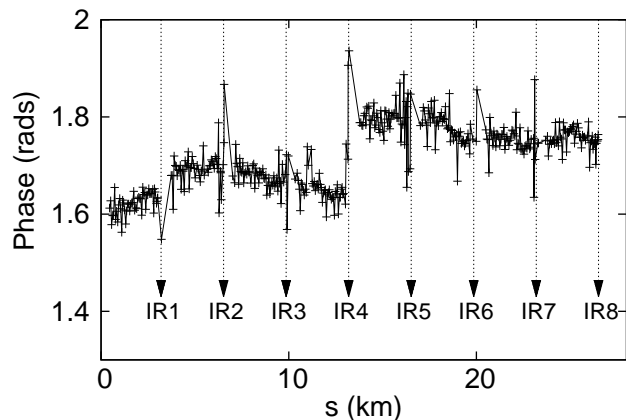


FIG. 2. Phase of an average trajectory that was obtained using the lattice functions with errors. The average trajectory was built from an experimental TBT data set of beam 2. Phase measurements in or near the IRs are not used since they have much larger fluctuations than phase measurements in the arcs. The AC dipole is responsible for the jump that can be seen in IR4.

To estimate J_c and δ_c from experimental data and evaluate their accuracies, action and phase plots are obtained from LHC experimental TBT data using the lattice functions with errors. It can be seen that these plots are almost constant for both beams and planes except for jumps at the AC dipole location. These jumps are particularly strong in the x -plane of beam 2 (see Fig. 2). Jumps in action and phase plots are due to differences between the real model and the model that is actually used to obtain these plots. The lattice functions used to obtain Fig. 2 do not include the effect of the AC dipole. Therefore, jumps are expected at this location.

Having jumps in the middle of the action and phase plots is not convenient since it limits the number of BPMs

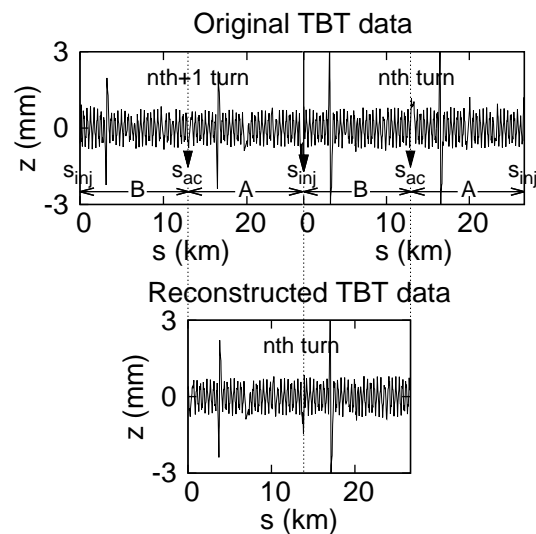


FIG. 3. Reconstruction of the n th turn from the n th + 1 and n th turns of a TBT data set. The n th turn of the reconstructed TBT data set is made of segment “A” of the original n th + 1 turn and segment “B” of the original n th turn. In this way, the reconstructed turn begins and ends at the longitudinal position of the AC dipole s_{ac} . The segments “A” and “B” are determined by s_{ac} and the longitudinal position of the injection point s_{inj} as shown in the figure.

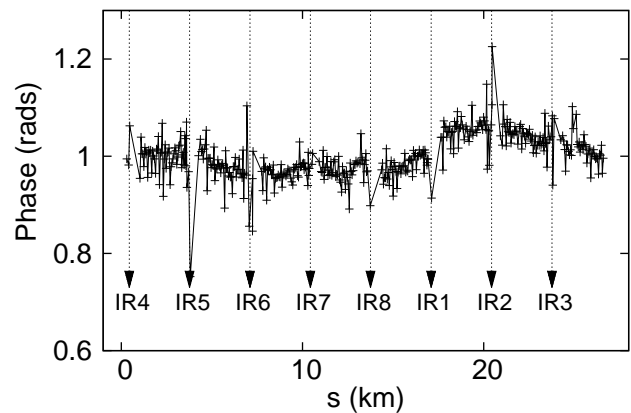


FIG. 4. Phase of an average trajectory obtained from the new TBT data set resulting from the reassignment of the longitudinal position of the original TBT data set used in Fig. 2. The longitudinal position of $\beta_r(s)$ and $\psi_r(s)$ were also reassigned accordingly. Now it is possible to use all phase measurements (more than 400) to estimate δ_c .

that can be used to estimate J_c and δ_c . Fortunately, the longitudinal position originally assigned to the elements of the accelerator lattice can be reassigned so that the start and end points of the action and phase plots correspond to the location of the AC dipole. In this way, the AC dipole jump moves toward the edge of the plots.

The reassignment of the longitudinal position must be performed for all measurements and functions that are used to generate the action and phase plots, which are the

BPM measurements, $\beta_r(s)$, and $\psi_r(s)$. To reassign the longitudinal position of the BPMs measurements, every turn of a given TBT data set should be reconstructed as illustrated in Fig. 3.

Reassignment of the longitudinal position of the β -functions is done according to the difference between the injection location and the AC dipole location. Reassignment of the longitudinal position of the betatron phase functions are similar to that of the β -functions but, in addition, the term $2\pi Q$ (with Q the natural betatron tune) must be subtracted from the original phases in the segment ‘‘A’’ (see Fig. 3). After applying APJ analysis to the same TBT data set used in Fig. 2 and the same $\beta_r(s)$ and $\psi_r(s)$, but with the longitudinal position reassigned, no significant jumps appear as can be seen in Fig. 4.

Now it is possible to estimate J_c and δ_c with all available action and phase measurements as a simple average. The uncertainty associated with J_c and δ_c is equal to the corresponding standard deviation divided by the square root of the number measurements available in each case. The standard deviation for δ_c is not larger than 0.038 rads. Since the number of measurements is roughly 400, the uncertainty associated with δ_c is approximately 0.002 rads. The standard deviation for J_c is at most 10% of its average value, so the corresponding uncertainty is less than 0.5%.

V. FOUR-QUADRUPOLE CORRECTION FROM EXPERIMENTAL LHC DATA

The four-quadrupole correction was proposed and tested with only simulations in reference [6]. It is now possible to estimate the strengths for this kind of correction from experimental data thanks to the new method that allows finding J_t and δ_t with very low uncertainties.

The strengths are mainly obtained from one-turn beam trajectories. To generate this kind of trajectories, a beam consisting of a single bunch is excited transversally to large amplitudes using an AC dipole. This ensures that the beam circulates for thousands of turns without decoherence effects or significant growth of the bunch size [15]. In every turn, all available BPMs detect and measure the transverse position of the the bunch centroid, which results in a one-turn beam trajectory. Since the beam circulates for thousands of turns, thousands of one-turn trajectories are obtained every time the AC dipole is activated. All these trajectories are saved in a file, which is referred to as a TBT data set. In principle, only two one-turn trajectories are needed to make the strength estimates. However, the noise present in these trajectories can generate fluctuations in the corresponding action and phases plots as large as the action and phase jumps used to estimate the correction strengths. To solve this problem, special one-turn trajectories are built by selecting certain trajectories from the TBT data set and averaging them. This results in what is called an average trajectory, which is finally the one-turn trajectory that is used

to estimate correction strengths. The detailed procedure to build the average trajectories and the validity of using them can be found in [6].

Before estimating the correction strengths, it is necessary to estimate the quadrupole components of the equivalent kicks from the average trajectories. These estimates are made using Eqs. (15) to (18), Eq. (2) and Eq. (7), which leads to Table III.

TABLE III. Quadrupole components of the equivalent kicks due to magnetic errors in the left and right triplets of IR1. All values given in units of $10^{-4} m^{-1}$.

Left $B_{1x,e}$	-9.70 ± 0.04
Left $\hat{B}_{1y,e}$	-8.03 ± 0.06
Left $\hat{B}_{1x,e}$	-4.95 ± 0.05
Left $B_{1y,e}$	-7.15 ± 0.05
Right $B_{1x,e}$	9.73 ± 0.05
Right $\hat{B}_{1y,e}$	8.19 ± 0.06
Right $\hat{B}_{1x,e}$	7.91 ± 0.04
Right $B_{1y,e}$	9.93 ± 0.06

The experimental data used to obtain Table III consists of five TBT data sets of beam 1, five TBT data sets of beam 2, and k -modulation measurements for both beams (Table IV) that were taken in 2016. For these experiments, IR1 was configured with a nominal β^* of 40 cm, local and global coupling corrections were already implemented, but normal quadrupoles corrections were off. To obtain the statistical uncertainties shown in Table III, the same procedure was applied to every pair of TBT data sets (one TBT data set of beam 1 and one TBT data set of beam 2), which resulted in 5 different estimates for every quadrupole component. The uncertainty was calculated as three times the standard deviation of these 5 estimates.

TABLE IV. Values for the optical variables of the IR1 inter-triplet space obtained from k -modulation measurements.

	β_r^* (cm)	w_r (cm)	β_{w_r} (cm)
X - B1	86.1	43.0	40.7
Y - B1	70.3	33.8	44.9
X - B2	57.9	27.4	38.2
Y - B2	70.0	35.2	39.7

Once the quadrupole components of the equivalent kicks are known, Eq. (11) can be used to estimate the correction strengths from either beam 1 TBT data (method A) or from beam 2 TBT data (method B), which leads to Table V. The magnets used in the correction correspond to two quadrupoles of the left IR1 triplet (Q2L and Q3L) and two quadrupoles of the right IR1 triplet (Q2R and Q3R). Since these quadrupoles are common to both beams, correction strengths obtained from either beam 1 or beam 2 data should be identical. However, the resulting correction strengths are different for each

TABLE V. Correction strengths obtained after applying Eq. (11) on beam 1 experimental TBT data (method A) and beam 2 experimental TBT data (method B). The same procedure used in Table III is used to obtain the statistical uncertainties shown.

Magnet	Correction strengths ($10^{-5} m^{-2}$)	
	A	B
Q2L	1.28 ± 0.01	1.20 ± 0.02
Q2R	-0.97 ± 0.02	-0.70 ± 0.01
Q3L	1.83 ± 0.02	1.07 ± 0.03
Q3R	-2.96 ± 0.04	-2.56 ± 0.02

case (columns A and B of Table V). These differences are significantly larger than the statistical uncertainties in Table V, specially for quadrupole Q3L. The presence of magnetic errors in the matching quadrupoles can explain these differences since these quadrupoles are no common to both beams. For this reason, a more general correction that takes into account the matching quadrupoles was developed, and it is presented in the following section.

VI. CORRECTIONS IN THE MATCHING SECTIONS

As mentioned earlier, the matching quadrupoles are located just outside the triplets and there are two sets of these quadrupoles per triplet (one per each beam), which leads to a total of 4 sets per IR. Each set has magnets identified with labels Q4, Q5, Q6, etc. In most cases, the matching quadrupoles have betatron phases that are very similar between them and their corresponding triplet quadrupoles. Therefore, they are mathematically equivalent to triplet quadrupoles and hence the same procedure used to find Eq. (9) can be used to find expressions that relate the quadrupole components of the equivalent kicks with their correction strengths. Since the matching quadrupoles of beam 1 are independent of the matching quadrupoles of beam 2, independent expressions must be derived for each beam leading to a system of four equations. For the left IR1 side, those

equations are

$$B_{1x,e} = -\frac{\Delta K_{1a}I_{x,a} + \Delta K_{1b}I_{x,b} + \Delta K_{1c}I_{x,c}}{\beta_{n,x}(s_e)} - \frac{\Delta K_{1d}I_{x,d}}{\beta_{n,x}(s_e)}, \quad (19a)$$

$$B_{1y,e} = -\frac{\Delta K_{1a}I_{y,a} + \Delta K_{1b}I_{y,b} + \Delta K_{1c}I_{y,c}}{\beta_{n,y}(s_e)}, \quad (19b)$$

$$\hat{B}_{1x,e} = -\frac{\Delta K_{1a}\hat{I}_{x,a} + \Delta K_{1b}\hat{I}_{x,b} + \Delta \hat{K}_{1c}\hat{I}_{x,c}}{\hat{\beta}_{n,x}(s_e)}, \quad (19c)$$

$$\hat{B}_{1y,e} = -\frac{\Delta K_{1a}\hat{I}_{y,a} + \Delta K_{1b}\hat{I}_{y,b} + \Delta \hat{K}_{1c}\hat{I}_{y,c}}{\hat{\beta}_{n,y}(s_e)} - \frac{\Delta \hat{K}_{1d}\hat{I}_{y,d}}{\hat{\beta}_{n,y}(s_e)}, \quad (19d)$$

where a and b correspond to the triplet magnets Q2 and Q3, and c and d correspond to the matching magnets Q4 and Q6. Q5 does not appear because its effect on the correction is equivalent to the effect of Q4 except for a scale factor; therefore, only Q4 needs to be activated. Other quadrupoles of the IR does not appear because their beta functions are significantly lower than the beta functions of quadrupoles Q1 to Q6. It should also be noted that Q6 does not appear in Eqs. (19b) and (19c). The corresponding terms have beta functions and integrals that are very small and, therefore, can be neglected.

The circumflex is used to distinguish the variables of beam 2 from those corresponding to beam 1. Since magnets a and b are common to both beams, no distinction should be made between beam 1 and beam 2 for the correction strengths associated with these magnets.

There are 4 equations and 6 variables in Eq. (19); therefore, there are infinite possible solutions. A possible solution can be found if the strengths of all no common correctors are initially forced to zero and the strengths of the common correctors are fitted to the resultant equations. Once ΔK_{1a} and ΔK_{1b} are found, they can be substituted in the original set of equations, and a linear system of four-by-four equations is obtained, which can be solved by conventional methods.

The equations for the right side of IR1 are

$$B_{1x,e} = -\frac{\Delta K_{1a}I_{x,a} + \Delta K_{1b}I_{x,b} + \Delta K_{1c}I_{x,c}}{\beta_{n,x}(s_e)}, \quad (20a)$$

$$B_{1y,e} = -\frac{\Delta K_{1a}I_{y,a} + \Delta K_{1b}I_{y,b} + \Delta K_{1c}I_{y,c}}{\beta_{n,y}(s_e)} - \frac{\Delta K_{1d}I_{y,d}}{\beta_{n,y}(s_e)}, \quad (20b)$$

$$\hat{B}_{1x,e} = -\frac{\Delta K_{1a}\hat{I}_{x,a} + \Delta K_{1b}\hat{I}_{x,b} + \Delta \hat{K}_{1c}\hat{I}_{x,c}}{\hat{\beta}_{n,x}(s_e)} - \frac{\Delta \hat{K}_{1d}\hat{I}_{x,d}}{\hat{\beta}_{n,x}(s_e)}, \quad (20c)$$

$$\hat{B}_{1y,e} = -\frac{\Delta K_{1a}\hat{I}_{y,a} + \Delta K_{1b}\hat{I}_{y,b} + \Delta \hat{K}_{1c}\hat{I}_{y,c}}{\hat{\beta}_{n,y}(s_e)}, \quad (20d)$$

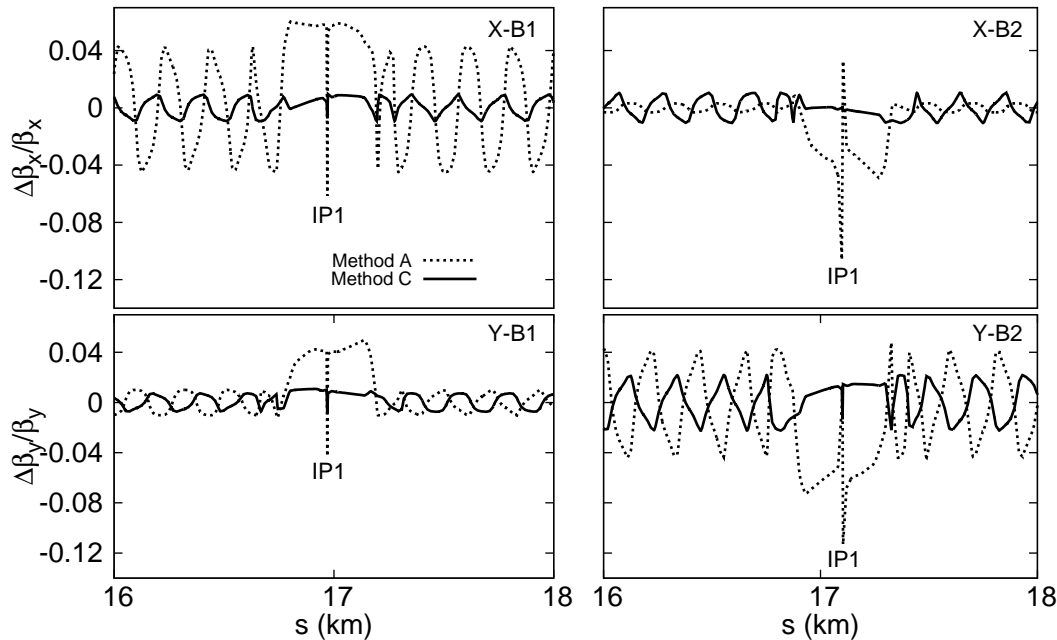


FIG. 5. β -beating for the magnetic error distribution plus the corrections shown in Table VI. The residual β -beating after applying common corrector are represented by dotted lines. The residual β -beating after applying all correctors are represented by solid lines. The dotted lines are obtained with correction strengths estimated with method A. Similar results are obtained with method B.

which are solved following the same procedure employed for Eq. (19). After solving Eqs. (19) and (20), a total 12 correction strengths can be found for the IR.

The validity of Eqs. (19) and (20) can be tested through simulated TBT data generated by MADX in a LHC lattice with a magnetic error distribution that includes magnetic errors in the matching quadrupoles. This magnetic error distribution is created as realistically as possible (first column of Table VI). For this purpose, the magnetic error distribution is chosen so that its equivalent quadrupole components $B_{1z,e}$ are close to their corresponding experimental values. This does not necessarily mean that the magnetic error distribution corresponds to the actual error distribution. Due to degeneracy, there are infinite possible error distributions that reproduce the experimental $B_{1z,e}$. Using the simulated TBT data generated with the error distribution shown in the first column of Table VI, the strengths for a twelve-quadrupole correction are estimated, which results in the last column (method C) of Table VI. The corresponding residual β beating (errors plus corrections), shown with the solid lines in Fig. 5, is below 4% throughout the ring, including the IP. The strengths of a four-quadrupole correction are also estimated with data from beam 1 (method A) and beam 2 (method B), leading to columns A and B of Table VI.

Correction strengths obtained by method A or method B can reduce the β -beating to acceptable levels in the arcs, but the β -beating in the IP can still be significant as shown by the dotted lines in Fig. 5. With the method presented in this section (method C), the residual β -beating in the arcs after applying this correction is smaller than with methods A and B, but more importantly, the residual β -beating at the IP is significantly reduced.

The strengths of a six-quadrupole (all triplet quadrupoles) correction were also obtained for the same error distribution using the SBS method [16]. The corresponding residual β beating is very similar to that found with method A or B, that is, it is acceptable in the arcs but very large in the IP.

VII. TWELVE-QUADRUPOLE CORRECTION FROM EXPERIMENTAL DATA AND COMPARISONS

The same experimental data used in Sec. V is used in this section to obtain the strengths of the twelve-quadrupole correction. The quadrupole components of the equivalent kicks for these data were already estimated in that section and correspond to Table III. Correction strengths are estimated by applying the procedure in the

TABLE VI. Strengths for a four-quadrupole correction estimated from beam 1 data (method A) and beam 2 data (method B). Also, the strengths for a twelve-quadrupole correction are shown in the last column (method C). The suffixes B1 and B2 are used to distinguish the quadrupoles of beam 1 from the quadrupoles of beam 2

Magnet	Magnetic error ($10^{-5} m^{-2}$)	Correction strengths ($10^{-5} m^{-2}$)		
		A	B	C
Q1L	-0.60	—	—	—
Q1R	0.70	—	—	—
Q2L	-1.17	1.17	1.00	1.08
Q2R	0.74	-0.92	-0.62	-0.77
Q3L	-1.31	1.90	1.21	1.55
Q3R	2.60	-2.97	-2.62	-2.79
Q4L.B1	-7.00	—	—	10.92
Q4L.B2	7.00	—	—	-10.94
Q4R.B1	5.70	—	—	-7.30
Q4R.B2	-5.70	—	—	7.31
Q5L.B1	-6.86	—	—	—
Q5L.B2	7.01	—	—	—
Q5R.B1	2.98	—	—	—
Q5R.B2	-3.45	—	—	—
Q6L.B1	41.34	—	—	-38.45
Q6L.B2	-31.51	—	—	32.02
Q6R.B1	-23.71	—	—	22.05
Q6R.B2	20.44	—	—	-19.32

previous section to those quadrupole components. The results are recorded in Table VII.

A comparison of the correction obtained in Table VII can be made with a six-quadrupole correction estimated with SBS, the method currently used in the LHC. In this method, a variable related to the betatron phase called the phase error is defined. This variable is equal to zero at some axial location just before the IR and starts to change as a function of the axial coordinate due to the magnetic errors in the IR. Experimentally, the phase error is obtained from Fourier analysis of TBT data and the corresponding simulated phase error is derived from MADX simulations. To find the correction strengths, the six quadrupoles that participate in the correction are varied iteratively until the simulated phase error coincides with the corresponding experimental phase error. The variables obtained from k-modulation (w_r , β_{w_r} and β^*) and the β -beating in the IR also participate in this iteration process.

A comparison based simply on correction strengths may not be adequate due to degeneracy. A more reliable method to compare two different correction should be based on their quadrupole components as explained in Appendix A. To make this comparison, the correction strengths obtained in Table VII are directly substituted in Eqs. (19), (20) and (8) to obtain the first column of Table VIII. As expected, the $B_{1z}^{(c)}$ are very close to the corresponding $B_{1z,e}$ obtained in Table III and also they have opposite signs so that they can cancel each other. The same procedure is applied to the correc-

TABLE VII. Correction strengths estimated for IR1 from 2016 LHC data. The same procedure used in Table III is used to obtain the statistical uncertainties shown.

Magnet	Correction strengths ($10^{-5} m^{-2}$)
Q2L	1.24±0.01
Q2R	-0.83±0.01
Q3L	1.45±0.02
Q3R	-2.76±0.02
Q4L.B1	11.0 ±0.35
Q4L.B2	-11.0 ±0.35
Q4R.B1	-7.7 ±0.39
Q4R.B2	7.7 ±0.39
Q6L.B1	-40.1 ±1.3
Q6L.B2	33.4 ±1.1
Q6R.B1	24.2 ±1.4
Q6R.B2	-21.2 ±1.2

tion strengths obtained from the SBS method (Table II of [7]) leading to the last column of Table VIII. An average difference of about 20% can be observed between the absolute values of the quadrupole components of both corrections. An explanation of these differences may be in the type of quadrupoles used in each correction. SBS only uses triplet quadrupoles, while APJ also uses triplet and matching quadrupoles.

TABLE VIII. The quadrupole components of the equivalent kicks due to the correction strengths are estimated for two different methods of corrections. All values are given in units of $10^{-4} m^{-1}$.

	APJ correction	SBS correction
Left $B_{1x}^{(c)}$	9.701	6.707
Left $\hat{B}_{1y}^{(c)}$	8.025	6.707
Left $\hat{B}_{1x}^{(c)}$	4.953	5.454
Left $B_{1y}^{(c)}$	7.152	5.454
Right $B_{1x}^{(c)}$	-9.726	-6.055
Right $\hat{B}_{1y}^{(c)}$	-8.186	-6.055
Right $\hat{B}_{1x}^{(c)}$	-7.914	-8.541
Right $B_{1y}^{(c)}$	-9.926	-8.541

When only triplet quadrupoles are used for correction, the quadrupole components of the equivalent kick due to the correction strengths are always subject to

$$B_{1x}^{(c)} \approx \hat{B}_{1y}^{(c)}, \quad (21)$$

$$B_{1y}^{(c)} \approx \hat{B}_{1x}^{(c)}, \quad (22)$$

as demonstrated in [6]. These symmetry relations can be clearly seen in the quadrupole components generated by the SBS correction (last column of Table VIII). In contrast, the experimental quadrupole components do not show these symmetries and, therefore, can not be completely compensated with a correction that only uses triplet quadrupoles.

SBS corrections during the 2016 LHC were considered essential to achieve a rms β -beating below 2% around the rings. But achieving this low β -beating does not necessarily imply that SBS corrections perfectly compensate the magnetic errors in the IRs; there is also the possibility that the global correction that was applied later through the matching and dispersion suppressor quadrupole also compensated the residual β -beating left by SBS corrections in every IR.

VIII. CONCLUSIONS

Mathematical relationships that allow estimating the action and phase in the inter-triplet space were deduced. It was shown that the uncertainties associated with these formulas were significantly lower than the uncertainties of a method that uses two BPMs in the inter-triplet space. This last method required a very precise calibration of the BPMs, which is not yet available in the LHC. In contrast, the new method can be used to make reliable estimates of action and phase in the inter-triplet space with the hardware currently available in the LHC.

Strengths of a four-quadrupole correction for IR1 were estimated from experimental LHC data. These strengths were estimated independently for each beam giving different values, suggesting that magnetic errors in the no common quadrupoles of the IR were significant. As a consequence, a more general correction scheme that uses twelve quadrupoles was developed and tested with simulations. These simulations show that the twelve-quadrupole correction can suppress the β beating generated in the IR throughout the ring, including the IP, even when there are large magnetic errors in the matching quadrupoles. In contrast, the four-quadrupole and six-quadrupole correction, either estimated with APJ or SBS, cannot guarantee suppression of the β beating in the IP under these conditions.

The strengths of a twelve-quadrupole correction in IR1 were also estimated from LHC experimental data. The resulting correction was compared to a correction obtained in similar conditions with the SBS method. The comparison was made through the quadrupole components associated with the corrections obtained with each method. An average difference of 20% was found between the quadrupole components associated with each method. The fact that the SBS correction does not use the matching quadrupole as correctors, only the triplet quadrupoles, probably explains these differences. The SBS correction is acceptable if the residual β -beating is subsequently suppressed through global corrections as it is currently done in the LHC. If full local compensation is required, the matching quadrupole should be included in the correction as proposed in this paper.

The IR corrections in the LHC Run 3 in 2021 are expected to be significantly different to the corrections found during the LHC Run 2 or the LHC Run 1. The method presented in this paper is a viable option to re-

calculate those corrections.

ACKNOWLEDGMENTS

We are very thankful to all members of the optics measurement and correction team (OMC) at CERN for support with their k -modulation software, GetLLM program, and experimental data. Special thanks goes to Hector García Morales, member of the OMC team, for analysis of simulations related with the SBS correction method. Y. Rodríguez wants to thank the support received through “CONVOCATORIA NACIONAL PARA EL APOYO A LA MOVILIDAD INTERNACIONAL DE LA UNIVERSIDAD NACIONAL DE COLOMBIA 2017-2018”, which made possible a short stay at CERN.

Appendix A: Degeneracy in the Corrections

The quadrupole strengths of at least two quadrupoles in a triplet must be changed to suppress the quadrupole component of the equivalent kick associated with that triplet, as indicated in Sec. II. This suppression can also be done by changing the strengths of the three quadrupoles. In that case, Eqs. (8) and (9) becomes

$$B_{1x}^{(c)} = \frac{1}{\beta_{n,x}(s_e)} (\Delta K_{1a} I_{x,a} + \Delta K_{1b} I_{x,b} + \Delta K_{1c} I_{x,c}) \quad (\text{A1})$$

$$B_{1y}^{(c)} = \frac{1}{\beta_{n,y}(s_e)} (\Delta K_{1a} I_{y,a} + \Delta K_{1b} I_{y,b} + \Delta K_{1c} I_{y,c}).$$

Since there are 3 quadrupoles whose strengths can be changed and only two equations, there are infinite possible ways of generating the same quadrupole components. On the other hand, the β -beating generated by the correctors in the triplets is given by

$$\left(\frac{\Delta\beta_x(s)}{\beta_x(s)} \right)_{TR} = - \frac{\cos [2|\psi_{n,x}(s) - \psi_{n,x}(s_e)| - 2\pi Q_x]}{2 \sin 2\pi Q_x} \times \beta_{n,x}(s_e) B_{1x}^{(c)}, \quad (\text{A2})$$

$$\left(\frac{\Delta\beta_y(s)}{\beta_y(s)} \right)_{TR} = - \frac{\cos [2|\psi_{n,y}(s) - \psi_{n,y}(s_e)| - 2\pi Q_y]}{2 \sin 2\pi Q_y} \times \beta_{n,y}(s_e) B_{1y}^{(c)},$$

where Eq. (D4) of [6] was used. Since the β -beatings are proportional to the quadrupole components, there are infinite sets of correction strengths that generate the same β -beatings. This means that corrections with very different correction strengths can have the same effect in the accelerator optics. Therefore, if a comparison between two different corrections is required, it should be done

by comparing their quadrupole components instead of their individual correction strengths. This demonstration

can also be extended for the case in which the matching quadrupoles are also used in the correction.

-
- [1] M. Aiba, S. Fartoukh, A. Franchi, M. Giovannozzi, V. Kain, M. Lamont, R. Tomás, G. Vanbavinckhove, J. Wenninger, F. Zimmermann, R. Calaga, and A. Morita, *Phys. Rev. ST Accel. Beams* **12**, 081002 (2009).
- [2] R. Tomás, O. Brüning, M. Giovannozzi, P. Hagen, M. Lamont, F. Schmidt, G. Vanbavinckhove, M. Aiba, R. Calaga, and R. Miyamoto, *Phys. Rev. ST Accel. Beams* **13**, 121004 (2010).
- [3] R. Tomás, T. Bach, R. Calaga, A. Langner, Y. I. Levisen, E. H. Maclean, T. H. B. Persson, P. K. Skowronski, M. Strzelczyk, G. Vanbavinckhove, and R. Miyamoto, *Phys. Rev. ST Accel. Beams* **15**, 091001 (2012).
- [4] G. Vanbavinckhove, *Optics measurements and corrections for colliders and other storage rings*, PhD dissertation, Universiteit van Amsterdam (2012).
- [5] J. F. Cardona, *Linear and Non Linear Studies at RHIC Interaction Regions and Optical Design of the Rapid Cycling Medical Synchrotron*, PhD dissertation, Stony Brook University, Department of Physics (2003).
- [6] J. F. Cardona, A. C. García Bonilla, and R. Tomás García, *Phys. Rev. Accel. Beams* **20**, 111004 (2017).
- [7] T. Persson, F. Carlier, J. Coello de Portugal, A. Garcia-Tabares Valdivieso, A. Langner, E. H. Maclean, L. Malina, P. Skowronski, B. Salvant, R. Tomás, and A. C. García Bonilla, *PRAB* **20**, 061002 (2017).
- [8] H. Grote, F. Schmidt, L. Deniau, and G. Roy, *The MAD-X Program*, European Organization for Nuclear Research (2015).
- [9] J. F. Cardona and S. G. Peggs, *Phys. Rev. ST Accel. Beams* **12**, 014002 (2009).
- [10] F. Carlier and R. Tomás, *Phys. Rev. Accel. Beams* **20**, 011005 (2017).
- [11] P. Castro, *Luminosity and beta function measurement at the electron-positron collider ring LEP*, PhD dissertation, Universitat de Valencia (1996).
- [12] P. Skowroński, F. Carlier, J. C. de Portugal, A. Garcia-Tabares, A. Langner, E. Maclean, L. Malina, M. McAteer, T. Persson, B. Salvant, and R. Tomás, in *Proceedings of IPAC 2016* (2016).
- [13] A. Langner and R. Tomás, *Phys. Rev. ST Accel. Beams* **18**, 031002 (2015).
- [14] A. Wegscheider, A. Langner, R. Tomás, and A. Franchi, *Phys. Rev. Accel. Beams* **20**, 111002 (2017).
- [15] M. Bai, S. Y. Lee, J. W. Glenn, H. Huang, L. Ratner, M. J. Roser, T. and Syphers, and W. van Asselt, *Phys. Rev. E* **56**, 6002 (1997).
- [16] H. García, J. F. Cardona, and R. Tomás, “Apj vs sbs in ir,” <https://indico.cern.ch/event/850541/contributions/3578380/> (2019).